Combustion Chemistry of Enols: Possible Ethenol Precursors in Flames†

Craig A. Taatjes,* Nils Hansen, and James A. Miller

Combustion Research Facility, Mail Stop 9055, Sandia National Laboratories, Livermore, California 94551-0969

Terrill A. Cool and Juan Wang

School of Applied and Engineering Physics, Cornell University, Ithaca, New York 14853

Phillip R. Westmoreland and Matthew E. Law

Department of Chemical Engineering, University of Massachusetts, Amherst, Massachusetts 01003-9303

Tina Kasper and Katharina Kohse-Höinghaus

Physikalische Chemie I, Universität Bielefeld, Universitätsstrasse 25, 33615 Bielefeld, Germany

Received: August 22, 2005; In Final Form: October 13, 2005

Before the recent discovery that enols are intermediates in many flames, they appeared in no combustion models. Furthermore, little is known about enols' flame chemistry. Enol formation in low-pressure flames takes place in the preheat zone, and its precursors are most likely fuel species or the early products of fuel decomposition. The OH + ethene reaction has been shown to dominate ethenol production in ethene flames although this reaction has appeared insufficient to describe ethenol formation in all hydrocarbon oxidation systems. In this work, the mole fraction profiles of ethenol in several representative low-pressure flames are correlated with those of possible precursor species as a means for judging likely formation pathways in flames. These correlations and modeling suggest that the reaction of OH with ethene is in fact the dominant source of ethenol in many hydrocarbon flames, and that addition−elimination reactions of OH with other alkenes are also likely to be responsible for enol formation in flames. On this basis, enols are predicted to be minor intermediates in most flames and should be most prevalent in olefinic flames where reactions of the fuel with OH can produce enols directly.

Introduction

Recently enols, less stable tautomers of ketones and aldehydes, have been found to be intermediates in hydrocarbon flames.[1,2] Enols were postulated to be transient species by Erlenmeyer[3] in 1880, and the simplest enol, ethenol (vinyl alcohol, CH_2═CHOH), was not observed in the gas phase until 1976.[4] Given the historic elusiveness of the enols, it is not surprising that they have not been included in models of flame chemistry. Nevertheless, it is now evident that they are present in substantial concentrations in a wide range of flames. Ethenol was first observed in a rich ethene flame by Cool et al. in 2003,[2] and ethenol, propenols, and butenols were reported in a wide range of pure and mixed-fuel flames.[1]

Measurement of chemical compositions of flames is one of the foundations for the development of detailed chemical models of hydrocarbon oxidation. These models find application in many areas of science. They are critical for understanding pollutant formation and ignition phenomena in combustion[5,6] as highlighted and discussed in a recent review by Miller, Pilling, and Troe[7] They also are used as a basis for models of oxidation in supercritical water,[8] for representation of gas-phase chemistry in solid-oxide fuel cells,[9,10] and for descriptions of the hydrocarbon chemistry in planetary atmospheres.[11] Enols are minor components in flames, and their practical significance, if any, remains unclear. Explaining the presence of enols and their effects requires that combustion chemistry models be modified to include their formation and removal reactions. However, very little is known about the reactions of gas-phase neutral enols. Therefore, some guidance is required to determine which new reactions for enol production and consumption should be experimentally and computationally investigated for inclusion in detailed combustion chemistry mechanisms.

The concentrations of enols in flames are a result of the balance among production and removal reactions and transport, and detailed flame modeling will be required to establish the validity of any enol production mechanism. It is the aim of this work to describe the enol observations and analyze possible production reactions in the context of the measurements of other combustion intermediates. Previous work reported photoionization efficiency spectra showing enols in many flames, but detailed analysis of the enol chemistry had not proceeded beyond a single mole fraction profile, that of ethenol in a rich ethene flame. In the present work, mole fraction profiles are reported for ethenol in flames of ethene, allene, propene, cyclopentene, cyclohexane, and ethanol, along with an estimated mole fraction profile for propenols in a rich propene flame. Detailed modeling is carried out for allene, propyne, propene, methane, ethane, and ethene flames. The reaction of OH with C_2H_4 appears to dominate ethenol production in allene, ethanol, and ethene

† Part of the special issue "Jürgen Troe Festschrift".

* Author to whom correspondence should be addressed.

10.1021/jp0547313 CCC: $33.50
Published on Web 12/01/2005

TABLE 1: Flames Used in the Present Experiments

flame	pressure (torr)	feed fuel mole fraction	feed oxygen mole fraction	mass flux ($g\ m^{-2}\ s^{-1}$)
methane $\phi = 1.40$	31.0	0.182	0.260	66.5
ethene $\phi = 1.90$	30.0	0.217	0.343	20.7
ethane $\phi = 1.39$	30.0	0.141	0.354	18.6
ethanol $\phi = 1.96$	35.0	0.270	0.413	32.4
propene $\phi = 2.30$	37.6	0.254	0.495	38.3
allene $\phi = 1.80$	25.0	0.184	0.408	23.8
propyne $\phi = 1.80$	25.0	0.184	0.408	23.8
cyclopentene $\phi = 2.00$	37.6	0.166	0.581	44.1
cyclohexane $\phi = 1.00$	30.0	0.068	0.608	21.6

flames and plays a significant role in ethenol formation in cyclohexane and cyclopentene flames. Other reactions of OH with alkenes are also possible sources of enols, and it is suggested that OH + propene may be responsible for much of the enol production in rich propene flames.

Experiment and Model

The present experiments investigate low-pressure laminar premixed flames by molecular-beam mass spectrometry with photoionization by tunable vacuum ultraviolet light.[12−16] The experimental breakthrough that enabled detection of enols is the use of light from a third-generation synchrotron source, the advanced light source (ALS) at Lawrence Berkeley National Laboratory, for the ionization step.[1,2] The ease of tunability and good energy resolution of the synchrotron source facilitates discrimination of isomeric species based on their photoionization spectra. The full apparatus is described in more detail elsewhere.[17,18] It consists of a low-pressure flame chamber, a differentially pumped flame-sampling system, and a time-of-flight mass spectrometer. The 3-m monochromator at the chemical dynamics beamline of the ALS delivers a photon current of about 5×10^{13} photons s^{-1} with an energy resolution ΔE(fwhm) = 40 meV, as determined by measurements of narrow autoionization resonances of O_2. Higher undulator harmonics are suppressed by passing the undulator beam through a gas filter[19] filled with Ar or He. A NIST-calibrated silicon photodiode records the photon current.

A fuel/oxygen/Ar flame is stabilized on a translatable flat-flame (McKenna) burner of 6.03 cm diameter. The temperature in the flame is measured by a noncatalytically coated platinum/platinum−rhodium thermocouple, referenced to a calibration flame whose temperature has been measured by the sodium line-reversal method.[20] Flame gases are sampled through a 200 μm orifice in a fixed quartz cone mounted on a water-cooled flange. Translation of the burner relative to the cone allows sampling from different positions in the flame. The sampled gases pass through a nickel skimmer and cross the synchrotron beam. Pulsed-extraction time-of-flight mass spectrometry with a linear Wiley−McLaren[21] geometry is used to analyze the photoions. Spectra can be taken either as a function of burner position at a fixed photon energy or as a function of photon energy at a fixed burner position. The flame conditions for the flames described in this work are given in Table 1.

The measured photoion signals are normalized by the photon flux and corrected for background counts, fragmentation from higher-mass parents, contributions from isotopomers, and the mass discrimination of the molecular-beam sampling.[17] Mole fraction profiles are calculated using the protocol developed by Cool et al.[18] The mole fraction profile of Ar is computed from the measured Ar^+ signal at 16.65 eV photon energy, scaled by imposing element balance in the postflame zone (where gradients are small and diffusion effects can be neglected). Mole fractions of other species with known photoionization cross sections are then obtained by direct or indirect reference to Ar. Where photoionization cross sections are not known, they are estimated. In the present work the ionization cross section for ethenol versus photon energy is that estimated previously[2] and that for 1-propenol is taken to be the same as the estimated ethenol cross section, shifted by the difference in ionization energy. The overall uncertainty in the absolute mole fractions is estimated to range from approximately ±20% for major species, ±40% for ethenol, to about a factor of 2 for propenol. An improvement in accuracy may be possible with experimental changes, currently underway, to allow improved characterization of background contributions, especially that of H_2O. Relative mole fractions (i.e., the shapes of mole fraction profiles for a given species or relative peak mole fractions within a given flame) are significantly more accurate.

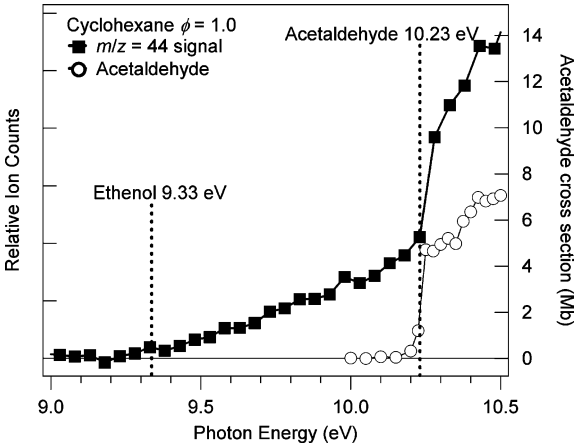

Figure 1. Photoionization efficiency curve for m/z = 44 from a stoichiometric cyclohexane flame, sampled with the probe 1.65 mm from the burner. The enol and keto tautomers can be clearly distinguished by their ionization energies, labeled with the vertical dotted lines. The photoionization efficiency of pure acetaldehyde is shown as the open symbols for comparison (1 Mb = 10^{-18} cm^2).

Identification of the enol isomers at a given mass is accomplished based on the differences in ionization energies with the keto tautomers.[1,2] Figure 1 shows the ion signal at m/z = 44, sampled from a stoichiometric (ϕ = 1.0) cyclohexane flame with the probe tip at 1.65 mm above the burner face, as a function of the photon energy. The ionization energies for the ethenol and acetaldehyde tautomers are labeled by vertical lines. The photoionization efficiency spectrum for the ethenol tautomer can be obtained by subtraction of a calibration spectrum of pure acetaldehyde.[2] Profiles of the individual tautomers can then be extracted from scans of ion signal versus height above burner at photon energies above and below the ionization threshold of acetaldehyde. Similar methods are applied to extract propenol profiles. In flames where comparisons to models are made, the experimental profiles are all shifted by a constant value in order to make the peak in the CH_3 mole fraction profiles coincide. Otherwise the distances from the burner given when reporting mole fractions in this paper are shifted toward the burner by 1 mm, 5 times the diameter of the sampling orifice, to approximately correct for sampling effects. However, the temperature profiles are all unperturbed temperature profiles.

The kinetic model used in the calculations is one that is constantly under development at Sandia. It has its origins in the work of Miller and Bowman,[22] Miller and Melius,[23] and Pope and Miller.[24] It has subsequently been modified and

TABLE 2: Possible Reactions of OH with Alkenes to Produce Enols

reaction	ΔH_{rxn} (298 K) (kcal mol^{-1})	ref
$OH + C_2H_4 \rightarrow CH_2CHOH + H$	+0.9	55−57
$OH + C_3H_6 \rightarrow CH_2CHOH + CH_3$	−7.8	55−57
$OH + C_3H_6 \rightarrow CH_3CH{=}C(OH)H + H$	−3.3	55, 56, 58
$OH + C_3H_6 \rightarrow CH_2{=}C(OH)CH_3 + H$	−3.8	55, 56, 59
$OH + CH_2CHCHCH_2 \rightarrow CH_2CHOH + C_2H_3$	+7.1	55−57, 60
OH + cyclopentene → $CH_2CHOH + C_3H_5$	−5.1	55−57, 61

extended based on the modeling of Skjøth-Rasmussen et al.,[25] the theoretical analyses of Miller, Klippenstein, and coworkers,[26−38] and the recent evaluations of Baulch et al.[39] In particular new computational results for the reaction of OH with ethene,[26] including the production of H + ethenol, have been incorporated into the model, as well as estimated values for removal reactions of ethenol. Unless otherwise indicated, the $OH + C_2H_4$ reaction is the only reaction producing ethenol in the model. The calculations were performed with CHEMKIN 4.0.3,[40] which allows for more flexibility in describing the pressure dependence of rate coefficients than previous versions of CHEMKIN.

Results and Discussion

Ethenol has been observed[1] in flames of benzene, propyne, allene, propene, ethene, 1,3-butadiene, cyclohexane, cyclopentene, ethanol, *n*-propanol, and gasoline. This work focuses principally on flames of a subset of these fuels that can be reliably modeled with the Sandia mechanism. Complete characterization of these flames will be reported in future publications; the present emphasis is on possible production reactions for ethenol and propenol. The highest observed ethenol mole fractions in these flames are on the order of 10^{-4}, and the peak in ethenol occurs near the bottom of the luminous zone in all flames where it has been observed.

Definitive assignment of the production mechanism for enols will require detailed flame modeling and accurate computation or measurement of the relevant rate constants. Chemical mechanisms of sufficient accuracy are not yet available for all the flames in which enols have been measured, and most of the relevant elementary reactions remain unstudied. The present work builds a case for several enol production pathways from comparisons of modeled and experimental mole fraction profiles of enols in representative flames, extended by consideration of correlations between mole fraction profiles of proposed precursors and that of ethenol. These simple correlations serve as qualitative guides. The reaction zone is neither isothermal nor a purely convective plug flow. The usual profile of a reactant and its product has the mole fraction of the product peaking downstream of the peak in the mole fraction of the precursor. This relationship does not always hold; if a product is thermally less stable than the reactant, for example, it may be consumed much nearer the burner than is the reactant. Correlations can also be obtained between mole fractions of precursors and products among flames of different fuels. For example, if ethene were the principal precursor of ethenol in flames of several fuels, one may expect more ethenol in the flames that contain more ethene.

The reaction of OH with ethene has been calculated to produce ethenol by chemically activated addition−decomposition,[26,41,42] and reactions of OH with other olefinic species may also produce enols. The thermochemistry of several candidate reactions is summarized in Table 2. Few experiments have been carried out on branching fractions for these reactions, and detailed calculations of energies for the relevant transition states are also absent from the literature, except for the case of OH + ethene. Theoretical and experimental characterization of these reactions would be very helpful in elucidating the formation chemistry of enols in flames. The following discussion considers which of these reactions are consistent with the flame observations.

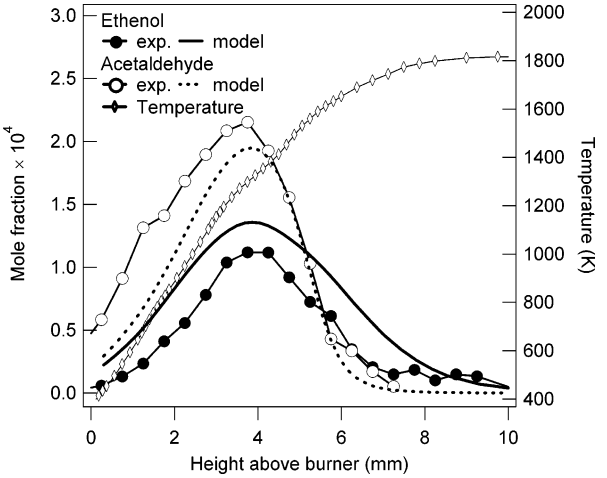

Figure 2. Experimental and modeled mole fraction profiles in a rich ($\phi = 1.9$) ethene flame. The experimental mole fraction profiles are shifted 1 mm closer to the burner than the probe−burner distance so that the peak positions of the modeled and experimental CH_3 mole fractions coincide. The unperturbed temperature profile is also shown.

OH + Ethene Reaction. The ethenol profile in a rich ($\phi = 1.9$) ethene flame has been successfully modeled,[1] and the dominant production mechanism of ethenol in this flame is the reaction of OH with C_2H_4, one product channel of which yields ethenol:

$$OH + C_2H_4 \xrightarrow{k_1} H + CH_2CHOH \qquad (1)$$

Reaction 1 is slightly (~1 kcal mol^{-1}) endothermic, and the reactants must traverse a barrier of 6 kcal mol^{-1} to reach the H + ethenol products,[26] but the reaction is rapid enough to produce substantial concentrations of ethenol. Calculations of the kinetics of this reaction[26,41,42] have predicted substantial branching to ethenol at temperatures above 1000 K. In the present model, the rate constant for reaction 1 is calculated[26] from the solution to the time-dependent master equation, using new ab initio characterization of stationary points on the OH−ethene potential energy surface. The rate coefficient for reaction 1 is approximately $k_1 = 1 \times 10^{-12}$ cm^3 molecule^{-1} s^{-1} near 1375 K and $k_1 = 2 \times 10^{-12}$ cm^3 molecule^{-1} s^{-1} near 1675 K, similar to the rate coefficient given by Hippler and Viskolcz,[42] but with a steeper temperature dependence. The new calculations also show that the $OH + C_2H_4$ reaction produces mainly $C_2H_3 + H_2O$ at high temperatures, with the branching into channel 1 of about 10% above 1250 K.[26] Details of the potential energy surface and calculated rate coefficients will be given in a separate publication.[26] The model using these calculated rate coefficients for reaction 1 as the only source of ethenol yields a peak rate of production of ethenol in the $\phi = 1.9$ ethene flame (given by $k_1[C_2H_4][OH]$) on the order of 10^{18} cm^{-3} s^{-1}. The experimental and modeled ethenol mole fractions in this flame are shown in Figure 2. Note that the model conditions used in a previous publication[1] were slightly too dilute (an Ar mole fraction of 0.5 instead of 0.44). The agreement between modeled and observed ethenol mole fractions is improved by correction of this error.

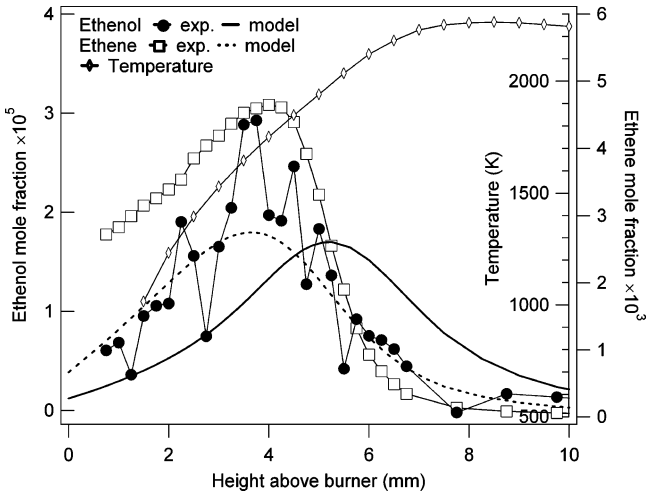

Figure 3. Measured and modeled mole fraction profiles for ethene and ethenol in a rich ($\phi = 1.8$) allene flame. The experimental profiles are shifted 0.25 mm closer than the burner−probe separation so that the peak positions of the modeled and experimental CH_3 mole fractions coincide. In the model ethenol is produced almost exclusively from the reaction of OH with ethene. The unperturbed temperature profile is also shown.

For the allene flame, modeling suggests that the entirety of the ethenol can be accounted for by the reaction of OH with C_2H_4. Figure 3 gives experimental and modeled mole fractions of ethene and ethenol in the allene flame. The model uses the same rate coefficients for OH + ethene as in the ethene flame model,[1,26] again as the sole source of ethenol in the flame. The model predicts the ethenol concentration in the rich allene flame relatively well; some of the discrepancy could arise from the $CH_3 + CH_2 \rightarrow H + C_2H_4$ reaction, whose rate constant is somewhat uncertain. The modeled peak in the ethenol mole fraction occurs beyond the peak in the ethene mole fraction, the usual relationship for a product and a precursor. The earlier peak of the ethenol relative to the model could reflect other sources of ethenol, but the amplitude is well-predicted by assuming reaction 1 as the sole ethenol source. Modeling of a propyne ($\phi = 1.8$) flame shows a similar ethenol profile and predicts the same formation mechanism, and measurements of the ethenol mole fraction in the propyne flame show similar agreement with the model.

In a previous report of enols in flames,[1] the $\phi = 2.0$ cyclopentene flame was shown to have the highest fraction of C_2H_4O as ethenol, that is, the largest ethenol/acetaldehyde ratio, of all flames studied thus far. However, the peak absolute mole fraction of ethenol, $\sim 5 \times 10^{-5}$, is substantially smaller than in the ethene ($\phi = 1.9$) flame, 1×10^{-4}. Investigation of the correlations between ethene and ethenol suggests that the reaction of OH and ethene is also the likely source of the ethenol in this flame. Figure 4 shows the mole fraction profiles of ethene and ethenol in the cyclopentene ($\phi = 2.0$) flame. The peak ethene mole fraction is nearly 3 times that in the allene flame, a bit larger than would be proportional to the approximately 2 times larger mole fraction of ethenol in the cyclopentene flame. However, cyclopentene is present in far greater concentrations than ethene, especially near the burner, and the reaction of cyclopentene with OH could conceivably form ethenol and the allyl radical. The mole fraction profile of the allyl radical, also shown in Figure 4, tracks that of the ethenol. The formation of allyl and ethenol from cyclopentene and OH is exothermic by approximately 5 kcal mol^{-1} (Table 1). The rate coefficient for the overall reaction of OH with cyclopentene is 5×10^{-11} cm^3 $molecule^{-1}$ s^{-1} at 298 K,[43] although it has not been measured

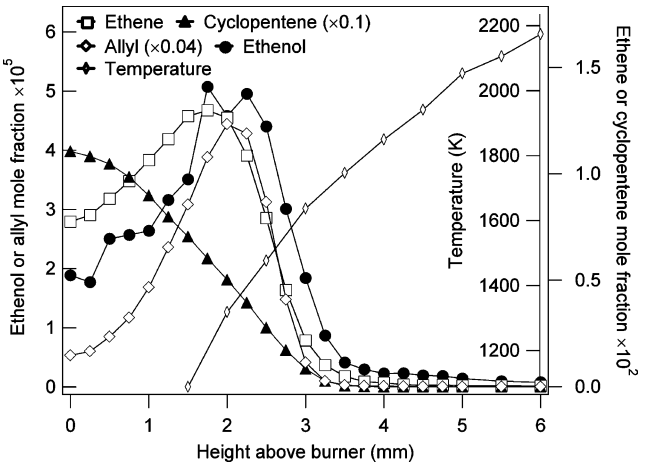

Figure 4. Mole fraction profiles in a rich ($\phi = 2.0$) cyclopentene flame. The mole fraction profiles are shifted 1 mm closer to the burner than the probe−burner distance as an approximate correction for sampling effects. The unperturbed temperature profile is also shown.

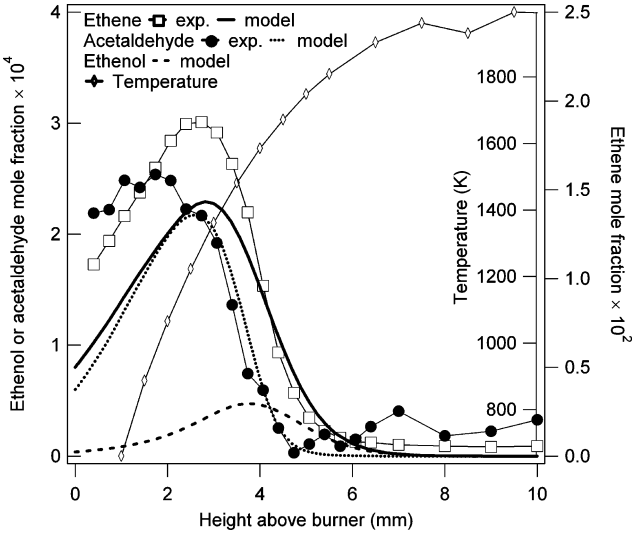

Figure 5. Experimental and modeled mole fractions in a $\phi = 1.4$ ethane flame. The experimental mole fraction profiles are shifted 1.5 mm closer to the burner than the probe−burner distance so that the peak positions of the modeled and experimental CH_3 mole fractions coincide. Despite high ethene mole fractions, the ethenol in this flame is below detection limits (less than $\chi = 10^{-5}$). The unperturbed temperature profile is also shown.

at higher temperature. Nevertheless, formation of ethenol and allyl following addition of OH to cyclopentene would require a convoluted rearrangement. Attempts to locate a transition state for this rearrangement have so far been unsuccessful, and there is no clear evidence that the reaction of OH and cyclopentene is a significant source of ethenol in the rich cyclopentene flame.

In the flames discussed above, the addition−elimination reaction of OH with ethene appears as one of the principal sources of ethenol. The fuel in these flames is either ethene itself or a fuel that produces relatively high concentrations of ethene in the preheat zone. It is worth investigating the contrasting case of rich flames of small alkane fuels, where the concentration of enols is below the detection limit of the present experiments (less than approximately a mole fraction of 10^{-5}),[1] yet the peak concentration of ethene is relatively high. Figure 5 shows the experimental and modeled ethene mole fraction profiles for a rich ($\phi = 1.4$) ethane flame. The peak ethene mole fraction is similar to that in the cyclopentene flame, and is 4−10 times larger than that in the allene or cyclohexane flames

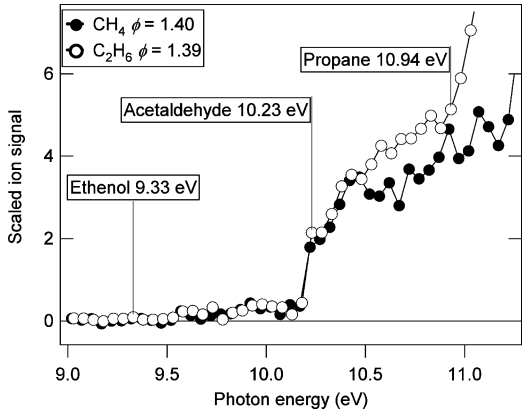

Figure 6. Photoionization efficiency spectra of $m/z = 44$ ions sampled from rich methane and ethane flames. No clear threshold can be observed at the ethenol ionization energy, and the upper bound on the ethenol mole fraction is 10^{-5} in both flames.

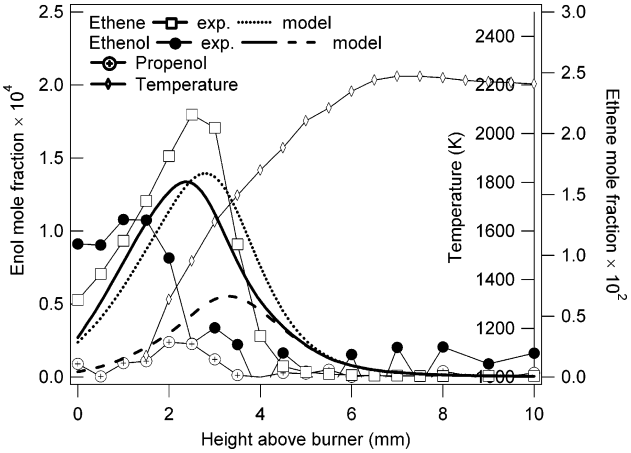

Figure 7. Mole fraction profiles from a rich ($\phi = 2.3$) propene flame. The mole fraction profiles are shifted 1.5 mm closer to the burner than the probe−burner distance so that the peak positions of the modeled and experimental CH_3 mole fractions coincide. The unperturbed temperature profile is also shown.

discussed above. Nevertheless, the photoionization efficiency spectra show no clear threshold that can be assigned to ethenol, as shown in Figure 6. An approximate upper limit of 10^{-5} is placed on the ethenol mole fraction in this flame, based on an estimated maximum ethenol fraction of 0.05 in the spectrum of Figure 6 and the measured total C_2H_4O profile. Similarly, an unsuccessful search for ethenol was carried out in a rich ($\phi = 1.4$) methane flame (Figure 6). The present data for this flame have not been completely evaluated, but a nearly identical flame ($\phi = 1.42$, 30 torr) was measured by Musick et al.[44] This flame has peak ethene mole fractions of approximately 10^{-3} at a position in the flame where the temperature is approximately 1400 K;[44] however, the OH concentration is relatively low in methane flames when the ethene concentration is high. The peak ethenol production rate in this flame, based on the temperature, OH, and ethene profiles of Musick et al.,[44] is less than 1×10^{17} cm^{-3} s^{-1}, more than an order of magnitude smaller than that of the $\phi = 1.9$ ethene flame. The upper limit on the ethenol mole fraction in this flame, 10^{-5}, is approximately 10 times smaller than the peak ethenol mole fraction in the rich ethene flame.

A relatively small OH concentration where the high ethene mole fractions occur may partially explain the low enol concentration in methane and ethane flames despite substantial amounts of ethene. Nevertheless, this explanation appears incomplete when compared with detailed models of these flames. As shown in Figure 5, modeling the rich ethane flame, using the same rate coefficients for OH + ethene, predicts peak ethenol mole fractions on the order of 5×10^{-5}, well above the experimentally estimated upper limit. The experimental acetaldehyde profile, on the other hand, is modeled relatively well. Attempts to model the $\phi = 1.42$ methane flame of Musick et al.[44] give relatively poor agreement with their experiments, but predict a similar peak mole fraction of ethenol, again well above the estimated detection limit. A more thorough experimental search for enols in alkane flames is justified. However, errors in modeling the removal of enols may also play a role in this discrepancy. A more rigorous understanding of the reactions of enols with common flame radicals (OH, H, CH_3) is clearly needed. These removal reactions of enols also help in determining their concentrations in flames, but their kinetics have never been measured. In the present model these removal reactions for ethenol have simply been estimated based on the reactions of the acetaldehyde tautomer.

OH + Propene Reaction. The propene ($\phi = 2.3$) flame has a relatively large peak mole fraction of ethenol but has a relatively smaller peak mole fraction of ethene. Figure 7 shows the mole fraction profiles for ethene and ethenol in this flame. As can clearly be seen in the figure, the ethenol peaks considerably closer to the burner than the ethene, reaching its highest mole fractions while the ethene is steeply increasing, opposite to the typical relationship of precursor and product. The modeled profiles of ethene and ethenol in this flame, under the assumption that OH + ethene is the sole source of ethenol, are shown as dotted and dashed lines in Figure 7. This model underestimates the ethenol concentration by about a factor of 2 and shows the typical precursor−product relationship, with ethene peaking nearer the burner than ethenol. In propene flames, one should consider whether reaction of OH with the fuel could be a principal route to enols. The propene mole fraction is still more than 0.1 at the burner positions where ethenol is present. Modifying the model to include production of ethenol from OH + propene (simply assuming a rate coefficient of 9.1×10^{-13} cm^3 molecule^{-1} s^{-1} for the channel yielding ethenol) gives the prediction shown by the solid line in Figure 7. Both the amplitude and the peak position of the ethenol are better predicted with a model that assumes some production from OH + propene.

Reliable rate coefficients for production of enols in the OH + propene reaction are not yet available. The overall kinetics of the reaction has been extensively studied, but there are few measurements of reaction products. Hoyermann and Sievert[45] used mass spectrometry to measure the products of this reaction at low pressure and room temperature. They noted several bimolecular channels, including methyl + C_2H_4O, which they assigned as acetaldehyde, and H + C_3H_6O, which they assigned as acetone. It is possible that these products are in fact the enols. At higher temperatures many researchers have presumed that the reaction forms water and the allyl radical.[46,47] However, if the reaction is similar to the reaction of OH with ethene, one may expect formation of ethenol and methyl radicals by C−C fission following addition to the central carbon. Furthermore, either formation of propen-2-ol by C−H fission following OH addition to the central carbon, or of 1-propenol following terminal addition, is thermodynamically possible (Table 2), analogous to the formation of ethenol in the reaction of OH with ethene. Figure 7 also shows the measured mole fraction of 1-propenol in the ($\phi = 2.3$) flame. The cross section for photoionization of propenol is approximated by analogy to the estimated cross section for ethenol[2] and is probably accurate to

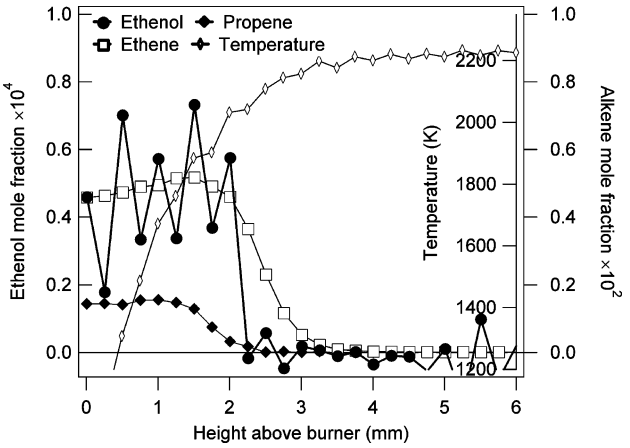

Figure 8. Mole fraction profiles from a $\phi = 1.0$ cyclohexane flame. The mole fraction profiles are shifted 1 mm closer to the burner than the probe−burner distance as an approximate correction for sampling effects, and the unperturbed temperature profile is shown.

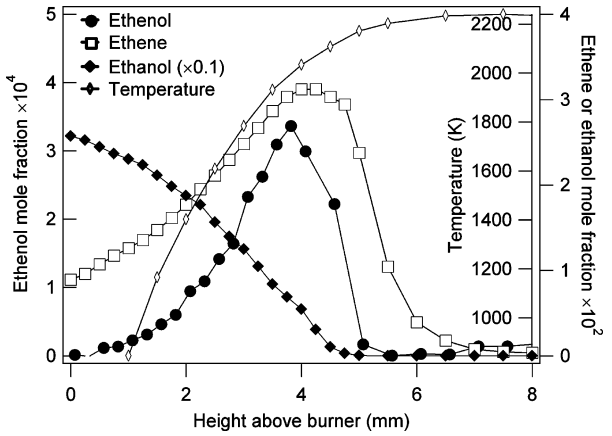

Figure 9. Mole fraction and temperature profiles from a $\phi = 1.97$ ethanol flame. The ethene mole fraction peaks slightly farther from the burner than does the ethenol mole fraction. The mole fraction profiles are shifted 1 mm closer to the burner than the probe−burner distance as an approximate correction for sampling effects. The unperturbed temperature profile is also shown.

no better than a factor of 2. At room temperature, Hoyermann and Sievert[45] measured the ratio of branching to the C_3H_6O channel to that of the C_2H_4O channel as 1:3.5. If a similar ratio occurs for relative branching to propenols and ethenol under flame conditions, the reaction of propene with OH appears as a likely source of the observed propenol in this flame. New measurements and detailed computational studies of branching fractions in the OH + propene reaction are plainly called for.

In the stoichiometric ($\phi = 1.0$) cyclohexane flame, the relationship of ethenol to ethene is similar to that in the rich allene flame. Figure 8 shows the mole fraction profiles for ethene and ethenol in this flame. One of the major destruction channels of cyclohexane proceeds through the cyclohexyl radical to $2C_2H_4 + C_2H_3$,[48] and the ethene mole fraction reaches $\sim 5 \times 10^{-3}$ in the preheat zone, about the peak mole fraction of ethene in the allene flame. The temperature near the peak of the ethene concentration is 1500−1600 K, which is similar to or slightly cooler than the temperature in the allene flame at the position of peak ethene concentration. If the loss of ethenol increases with increasing temperature, the losses may not be dissimilar in the two flames. However, the mole fraction of ethenol is approximately twice as large in the cyclohexane flame as in the allene flame. The reaction of OH with ethene is surely a major contributor to ethenol production in the $\phi = 1.0$ cyclohexane flame, but, as can be seen in Figure 8, the mole fraction of propene is also relatively large. It is possible that the reaction of OH with propene is also a substantial source of ethenol in this flame.

Dehydrogenation of Alcohols. Finally, in flames fueled by ethanol, it is conceivable that the mechanism for ethenol formation could include dehydrogenation of the fuel. Ruscic and Berkowitz[49] used dehydrogenation of ethanol in reactions with F atoms to produce ethenol. Pyrolysis of other alcohols has been shown to yield ethenol.[50] On the other hand, the abstraction of an H atom from ethanol by OH[51] and by H atoms[52] yields principally CH_3CHOH, which will likely form acetaldehyde rather than ethenol. Furthermore, whatever CH_2CH_2OH is formed will dissociate principally to ethene and OH, as in the "catalytic dehydration" of ethanol by OH noted by Hess and Tully.[53] Direct thermal dehydrogenation of ethanol faces very large barriers and is infeasible.[54] Mole fraction profiles of ethenol, ethene, and ethanol in a rich ($\phi = 1.96$) ethanol flame are displayed in Figure 9. The mole fraction of ethene is as great as that in other flames where models predict the OH + ethene reaction to be the dominant source of ethenol. The ethenol profile does peak somewhat closer to the burner than does ethene, albeit not in as dramatic a fashion as in the rich propene flame. This early peak of ethenol suggests an additional source of ethenol that does not rely on ethene; however, it might also merely reflect increased loss of ethenol in the higher-temperature region of the preheat zone. The temperature at the position of the peak in the ethene profile is 200−300 K higher in this rich ethanol flame than in the allene or cyclohexane flames. It appears that the reaction of OH with ethene may also suffice to predict ethenol formation in ethanol flames, although the evidence is not unambiguous.

Conclusions

The present results highlight the surprising room for improvement of realistic chemical models for combustion of even apparently simple fuels. Significant fundamental chemistry questions remain to be answered in order to assess the role of enols in flames. In general, reactions of OH with alkenes appear to be a key source of enols in the preheat zone of low-pressure flames. The overall rate coefficients for many of these reactions are well-known; however, experimental investigations of the product branching fractions, including their pressure dependence, are lacking. Detailed theoretical analysis of enol formation and removal reactions will be required to reliably model enol chemistry over a wide range of combustion conditions.

Acknowledgment. This work is supported by the Division of Chemical Sciences, Geosciences, and Biosciences, the Office of Basic Energy Sciences, the U.S. Department of Energy, in part under Grants DE-FG02-91ER14192 (P.R.W., M.E.L.) and DE-FG02-01ER15180 (T.A.C., J.W.), by the Chemical Science Division of the U.S. Army Research Office, and by the Deutsche Forschungsgemeinschaft under Ko 1363/18-1. Sandia is a multiprogram laboratory operated by Sandia Corporation, a Lockheed Martin Company, for the National Nuclear Security Administration under contract DE-AC04-94-AL85000. The Advanced Light Source is supported by the Director, Office of Science, Office of Basic Energy Sciences, Materials Sciences Division, of the U.S. Department of Energy under Contract No. DE-AC02-05CH11231 at Lawrence Berkeley National Laboratory. Ford Motor Company is gratefully acknowledged for supplying the propyne used in some of these experiments.

References and Notes

(1) Taatjes, C. A.; Hansen, N.; McIlroy, A.; Miller, J. A.; Senosiain, J. P.; Klippenstein, S. J.; Qi, F.; Sheng, L.; Zhang, Y.; Cool, T. A.; Wang, J.; Westmoreland, P. R.; Law, M. E.; Kasper, T.; Kohse-Höinghaus, K. *Science* **2005**, *308*, 1887.

(2) Cool, T. A.; Nakajima, K.; Mostefaoui, T. A.; Qi, F.; McIlroy, A.; Westmoreland, P. R.; Law, M. E.; Poisson, L.; Peterka, D. S.; Ahmed, M. *J. Chem. Phys.* **2003**, *119*, 8356.

(3) Erlenmeyer, E. *Chem. Ber.* **1880**, *13*, 305.

(4) Saito, S. *Chem. Phys. Lett.* **1976**, *42*, 399.

(5) Miller, J. A. *Proc. Combust. Inst.* **1996**, *26*, 461.

(6) Westbrook, C. K. *Proc. Combust. Inst.* **2000**, *28*, 1563.

(7) Miller, J. A.; Pilling, M. J.; Troe, J. *Proc. Combust. Inst.* **2005**, *30*, 43.

(8) Sullivan, P. A.; Ploeger, J. M.; Green, W. H.; Tester, J. W. *Phys. Chem. Chem. Phys.* **2004**, *6*, 4310.

(9) Naidja, A.; Krishna, C. R.; Butcher, T.; Mahajan, D. *Prog. Energy Combust. Sci.* **2003**, *29*, 155.

(10) Walters, K. M.; Dean, A. M.; Zhua, H.; Kee, R. J. *J. Power Sources* **2003**, *123*, 182.

(11) Ricca, A.; Bauschlicher, C. W., Jr.; Bakes, E. L. O. *Icarus* **2001**, *154*, 516.

(12) Werner, J. H.; Cool, T. A. *Chem. Phys. Lett.* **1998**, *290*, 81.

(13) Werner, J. H.; Cool, T. A. *Chem. Phys. Lett.* **1997**, *275*, 278.

(14) McIlroy, A.; Hain, T. D.; Michelsen, H. A.; Cool, T. A. *Proc. Combust. Inst.* **2000**, *28*, 1647.

(15) Werner, J. H.; Cool, T. A. *Combust. Flame* **2000**, *120*, 125.

(16) Werner, J. H.; Cool, T. A. *Combust. Flame* **1999**, *117*, 78.

(17) Cool, T. A.; McIlroy, A.; Qi, F.; Westmoreland, P. R.; Poisson, L.; Peterka, D. S.; Ahmed, M. *Rev. Sci. Instrum.* **2005**, *76*, 094102.

(18) Cool, T. A.; Nakajima, K.; Taatjes, C. A.; McIlroy, A.; Westmoreland, P. R.; Law, M. E.; Morel, A. *Proc. Combust. Inst.* **2005**, *30*, 1681.

(19) Suits, A. G.; Heimann, P.; Yang, X.; Evans, M.; Hsu, C.-W.; Lu, K.-t.; Lee, Y. T.; Kung, A. H. *Rev. Sci. Instrum.* **1995**, *66*, 4841.

(20) Bernstein, J. S.; Fein, A.; Choi, J. B.; Cool, T. A.; Sausa, R. C.; Howard, S. L.; Locke, R. J.; Miziolek, A. W. *Combust. Flame* **1993**, *92*, 85.

(21) Wiley, W. C.; McLaren, H. I. *Rev. Sci. Instrum.* **1955**, *26*, 1150.

(22) Miller, J. A.; Bowman, C. T. *Prog. Energy Combust. Sci.* **1989**, *15*, 287.

(23) Miller, J. A.; Melius, C. F. *Combust. Flame* **1992**, *91*, 21.

(24) Pope, C. J.; Miller, J. A. *Proc. Combust. Inst.* **2000**, *28*, 1519.

(25) Skjøth-Rasmussen, M. S.; Glarborg, P.; Østberg, M.; Larsen, M. B.; Sørensen, S. W.; Johnsson, S. E.; Jensen, A. D.; Christensen, T. S. *Proc. Combust. Inst.* **2002**, *29*, 1329.

(26) Senosiain, J. P.; Miller, J. A.; Klippenstein, S. J. The reaction of hydroxyl with ethylene. Submitted for publication. Preliminary results presented at the 4th Joint Meeting of the U.S. Sections of the Combustion Institute, Philadelphia, PA, March 20−23, 2005.

(27) Senosiain, J. P.; Klippenstein, S. J.; Miller, J. A. *J. Phys. Chem. A* **2005**, *109*, 6045.

(28) Klippenstein, S. J.; Miller, J. A. *J. Phys. Chem. A* **2005**, *109*, 4285.

(29) Senosiain, J. P.; Klippenstein, S. J.; Miller, J. A. *Proc. Combust. Inst.* **2005**, *30*, 945.

(30) Miller, J. A.; Klippenstein, S. J. *Phys. Chem. Chem. Phys.* **2004**, *6*, 1192.

(31) Miller, J. A.; Klippenstein, S. J. *J. Phys. Chem. A* **2003**, *107*, 7783.

(32) Miller, J. A.; Klippenstein, S. J. *J. Phys. Chem. A* **2003**, *107*, 2680.

(33) Miller, J. A.; Klippenstein, S. J. *J. Phys. Chem. A* **2002**, *106*, 9267.

(34) Klippenstein, S. J.; Miller, J. A.; Harding, L. B. *Proc. Combust. Inst.* **2002**, *29*, 1209.

(35) Miller, J. A.; Klippenstein, S. J. *Int. J. Chem. Kinet.* **2001**, *33*, 654.

(36) Hahn, D. K.; Klippenstein, S. J.; Miller, J. A. *Faraday Discuss.* **2001**, *119*, 79.

(37) Miller, J. A.; Klippenstein, S. J.; Robertson, S. H. *Proc. Combust. Inst.* **2000**, *28*, 1479.

(38) Miller, J. A.; Klippenstein, S. J.; Robertson, S. H. *J. Phys. Chem. A* **2000**, *104*, 7525.

(39) Baulch, D. L.; Bowman, C. T.; Cobos, C. J.; Cox, R. A.; Just, T. H.; Kerr, J. A.; Pilling, M. J.; Stocker, D.; Troe, J.; Tsang, W.; Walker, R. W.; Warnatz, J. *J. Phys. Chem. Ref. Data* **2005**, *34*, 757.

(40) Kee, R. J.; Rupley, R. M.; Miller, J. A.; Coltrin, M. E.; Grcar, J. F.; Meeks, E.; Moffat, H. K.; Lutz, A. E.; Dixon-Lewis, G.; Smooke, M. D.; Warnatz, J.; Evans, G. H.; Larson, R. S.; Mitchell, R. E.; Petzold, L. R.; Reynolds, W. C.; Caracotsios, M.; Stewart, W. E.; Glarborg, P.; Wang, C.; Adigun, O.; Houf, W. G.; Chou, C. P.; Miller, S. F.; Ho, P.; Young, D. J. *Chemkin*, release 4.0; Reaction Design, Inc.: San Diego, CA, 2004.

(41) Yamada, T.; Bozzelli, J. W.; Lay, T. *J. Phys. Chem. A* **1999**, *103*, 7646.

(42) Hippler, H.; Viskolcz, B. *Phys. Chem. Chem. Phys.* **2000**, *2*, 3591.

(43) Rogers, J. D. *Environ. Sci. Technol.* **1989**, *23*, 177.

(44) Musick, M.; van Tiggelen, P.; van Dooren, J. *Combust. Flame* **1996**, *105*, 433.

(45) Hoyermann, K.; Sievert, R. *Ber. Bunsen-Ges. Phys. Chem.* **1979**, *83*, 933.

(46) Wilk, R. D.; Cernansky, N. P.; Pitz, W. J.; Westbrook, C. K. *Combust. Flame* **1989**, *77*, 145.

(47) Tully, F. P.; Goldsmith, J. E. M. *Chem. Phys. Lett.* **1985**, *116*, 345.

(48) Law, M. E. Ph.D. Dissertation, University of Massachusetts, Amherst, MA, 2005.

(49) Ruscic, B.; Berkowitz, J. *J. Chem. Phys.* **1994**, *101*, 10936.

(50) Koga, Y.; Nakanaga, T.; Sugawara, K.-I.; Watanabe, A.; Sugie, M.; Takeo, H.; Kondo, S.; Matsumura, C. *J. Mol. Spectrosc.* **1991**, *145*, 315.

(51) Meier, U.; Grotheer, H. H.; Riekert, G.; Just, T. *Chem. Phys. Lett.* **1985**, *115*, 221.

(52) Park, J.; Xu, Z. F.; Lin, M. C. *J. Chem. Phys.* **2003**, *118*, 9990.

(53) Hess, W. P.; Tully, F. P. *Chem. Phys. Lett.* **1989**, *152*, 183.

(54) Park, J.; Zhu, R. S.; Lin, M. C. *J. Chem. Phys.* **2002**, *117*, 3224.

(55) Ruscic, B.; Wagner, A. F.; Harding, L. B.; Asher, R. L.; Feller, D.; Dixon, D. A.; Peterson, K. A.; Song, Y.; Qian, X.; Ng, C.-Y.; Lin, J.; Chen, W.; Schwenke, D. W. *J. Phys. Chem. A* **2002**, *106*, 2727.

(56) Afeefy, H. Y.; Liebman, J. F.; Stein, S. E. Neutral Thermochemical Data. In *NIST Chemistry WebBook, NIST Standard Reference Database Number 69*; Linstrom, P. J., Mallard, W. G., Eds.; National Institute of Standards and Technology: Gaithersburg, MD, June 2005; http://webbook.nist.gov.

(57) Holmes, J. L.; Lossing, F. P. *J. Am. Chem. Soc.* **1982**, *104*, 2648.

(58) Turecek, F.; Cramer, C. J. *J. Am. Chem. Soc.* **1995**, *117*, 12243.

(59) Turecek, F.; Havlas, Z. *J. Org. Chem.* **1986**, *51*, 4066.

(60) Ervin, K. M.; Gronert, S.; Barlow, S. E.; Gilles, M. K.; Harrison, A. G.; Bierbaum, V. M.; DePuy, C. H.; Lineberger, W. C.; Ellison, G. B. *J. Am. Chem. Soc.* **1990**, *112*, 5750.

(61) Ellison, G. B.; Davico, G. E.; Bierbaum, V. M.; DePuy, C. H. *Int. J. Mass Spectrom. Ion Processes* **1996**, *156*, 109.